Self-Assembled Monolayers on Mercury Probed in a Modified Surface Force Apparatus

Lucy Y. Clasohm,[†,‡,⊥] Miao Chen,[§] Wolfgang Knoll,[‡] Olga I. Vinogradova,[‡,||] and Roger G. Horn*[,†]

Ian Wark Research Institute, University of South Australia, Mawson Lakes, Adelaide SA 5095, Australia, Max-Planck-Institut für Polymerforschung, Postfach 3148, D-55021 Mainz, Germany, Lanzhou Institute of Chemical Physics, Chinese Academy of Sciences, Lanzhou 730000, People's Republic of China, and A. N. Frumkin Institute of Physical Chemistry and Electrochemistry, Russian Academy of Sciences, 31 Leninsky Prospect, 119991 Moscow, Russia

Received: April 16, 2006; In Final Form: October 11, 2006

Self-assembled monolayers (SAMs) of three thiol compounds formed on mercury are investigated by a combination of cyclic voltammetry, electrocapillary curves, and a novel method of measuring electrical double-layer properties. The last method involves a modified surface force apparatus in which a flat mica surface is pressed down toward a fixed mercury drop held beneath it, while both are immersed in aqueous electrolyte solution. Optical interference measurements are made of the mica−mercury separation as a function of electrical potential applied to the mercury, which yields information on the double-layer interaction between the two surfaces. Mercury is decorated by SAMs of 11-mercapto-1-undecanoic acid, which is shown to bring negative charge to the mercury/aqueous interface due to dissociation of the carboxylic acid groups; 11-mercapto-1-undecanol, which although it is uncharged changes the dipole potential of the interface; and 1-undecanethiol, which likewise changes the dipole potential, but by a different amount. The difference between the changes in dipole potential (90 mV) can be related to the different terminal groups of these two SAMs, $-CH_3$ compared to $-OH$, that are in contact with the aqueous phase.

1. Introduction

Studies of self-assembled monolayers (SAMs) of thiols on metals have attracted increasing interest in biology, colloid science, materials science, and microelectronic devices.[1−14] These SAMs are formed by spontaneous adsorption from a solution of organic molecules onto the surface of a solid, metal, or semiconductor immersed in the solution.[15] An organized SAM has a high degree of orientation, molecular order, and packing. SAMs formed from alkyl thiols, sulfides, and disulfides have been found to form densely packed, reproducible, and uniform SAMs on metals, through the strong sulfur−metal bond.[16] Most of the work in this area has involved SAMs made on gold surfaces,[3,11,12,15,17−22] mainly because gold is very inert and, hence, can be handled in ambient conditions. Other substrates that have been used include silver,[23−25] copper,[23,26,27] and various metal oxides.[13,28,29] However, pinholes are often observed in SAMs formed on solid substrates. Direct scanning tunneling microscopic images at different depths (on the surface of the monolayer and on the surface of the gold substrate) show that the pinholes in the SAM are caused by defects in the gold substrate.[30] These and other defects in the monolayer are crucial in many studies, having a major effect on phenomena such as electron transfer since their presence reduces the resistance of the film dramatically.

In this work, we investigate thiol SAMs formed on a mercury substrate. Being a liquid, it has a defect-free, renewable, and molecularly smooth surface, and it does not impose any crystalline spacing on the monolayers. Coupled with the inherent lateral mobility of the fluid substrate, these properties could allow SAMs incorporating appropriate biological molecules to make better biomimetic membranes than the tethered membranes currently formed on gold surfaces. Mercury can also be used as an ideally polarizable electrode for electrochemical investigations.

There are comparatively few studies on thiol SAMs on mercury. Demoz and Harrison[31] studied the influence of hexadecanethiol monolayers on a mercury surface on the electrochemical behavior of redox couples ($Ru(NH_3)_6^{2+/3+}$), and reported that an extremely impermeable, low-defect and high-density monolayer was formed. Cyclic voltammetry (CV) was used to examine the formation and organization of alkanethiols and ω-mercaptocarboxylic acid SAMs on mercury,[32] indicating that densely packed monolayers are formed. X-ray diffraction and reflectivity measurements[33,34] were also used to study the structure of alkanethiol films on mercury and showed that the monolayers are well aligned along the surface-normal direction and packed very densely at $\sim$19 Å^2/molecule. White and co-workers[35] studied the oxidative adsorption of *n*-alkanethiols on mercury in basic solutions and concluded that there are at least two chemical steps in monolayer formation. Two surface phases (low density and high density) were formed, and the transition between the two phases was shown to be potential-dependent. The surface charge density was measured as $\sigma = 95\ \mu C/cm^2$, which corresponds to a surface coverage of 9.8×10^{-10} mol/cm^2 ($\sim$17 Å^2/molecule) for the high-coverage phase. This result was confirmed by cyclic voltammetry and AC voltammetric studies of ω-mercaptocarboxylic acids on mercury,[14,36] where the adsorption of thiols is indicated to be controlled by either

* Corresponding author. E-mail: roger.horn@unisa.edu.au.
† University of South Australia.
‡ Max-Planck-Institut für Polymerforschung.
§ Chinese Academy of Sciences.
|| Russian Academy of Sciences.
⊥ Present address: Particulate Fluid Processing Centre, University of Melbourne, Parkville, Victoria 3010, Australia.

10.1021/jp062340y CCC: $33.50
Published on Web 11/30/2006

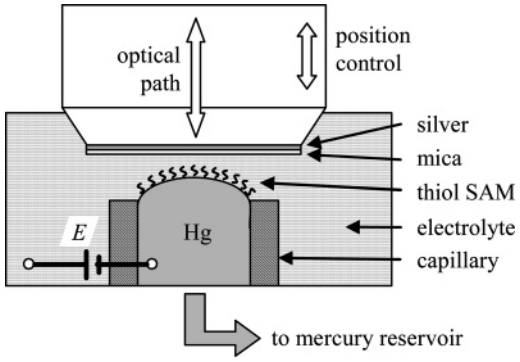

Figure 1. Schematic picture of the experiment.

physisorption or chemisorption, depending on the applied potential. The surface coverage measured by the reductive desorption of the SAMs of *n*-alkanethiolates from mercury in acetonitrile is 9.2×10^{-10} mol/cm^2 ($\sim$18 Å^2/molecule).[32] Moncelli's group used self-assembled lipids to form monolayers on mercury, intended for modeling biological membranes.[8,10,37−41] Whitesides' group[7,42] built metal−insulator−metal junctions based on SAMs to study the electron transport as a potential application in microelectronics.

A new technique that we introduce here for investigating SAMs on mercury is based on a recent development by Connor and Horn,[43−45] who modified a surface force apparatus (SFA) for the purpose of investigating physical interactions between a fluid drop and a solid surface immersed in an aqueous environment, including hydrodynamic interactions.[46−48] For more than a quarter of a century, the surface force apparatus has been an important tool for making direct force measurements, which have contributed enormously to our understanding of colloidal interactions. Most previous SFA measurements have been made with mica or other solid surfaces. However, the new development has enabled a modified SFA to investigate the deformation of a nonaqueous fluid drop interacting with a solid surface, and from this to derive information about electrical double-layer interactions between the two. This in turn gives information about the surface charge or potential at the fluid/water interface. Connor and Horn chose mercury for the fluid drop because its high reflectivity and the smoothness of its interface with water give excellent resolution in measuring the surface separation using a variation of the optical interference method ("FECO") that is central to the SFA technique. Furthermore, the conductivity of mercury allows its electrical potential, and hence surface charge, to be controlled by the experimenter, which gives control over the double-layer forces acting between it and the model solid, mica. Initial measurements between mercury and mica demonstrated the accuracy with which double-layer forces could be controlled and quantified.[46]

In this paper we report an extension of the mercury−SFA measurements to investigate the effect of modifying the mercury surface with adsorbed monolayers. SAMs of thiols with three different terminating groups (−COOH, −OH, and $-CH_3$) were investigated. The results to be presented below will show that the surface coated with carboxylic acid terminated SAM is negatively charged in aqueous solutions at natural pH. Although the −OH and $-CH_3$ SAMs are nominally uncharged, their presence and possible effect on adsorbed small ions from solution modify the structure of the inner double layer at a charged mercury surface, which has a significant effect on the double-layer interaction with mica by changing the dipole potential at the mercury/aqueous electrolyte interface.

The investigations of SAMs in the mercury−SFA have been augmented by two other measurements conducted in the SFA chamber, which assist in characterizing the formation and adsorption/desorption behavior of the thiols on mercury. The first is a study of the interfacial tension between the decorated mercury and the aqueous phase, by analyzing the shape of the mercury drop in a gravitational field (axisymmetric drop shape analysis), and the second is cyclic voltammetry. Results of these two methods for characterizing the SAMs will be presented first, before describing how additional information can be obtained from SFA measurements.

2. Experimental Methods

Figure 1 shows a schematic picture of how the experiment was arranged. A mercury drop protruded from a Kel-F capillary entering the bottom of a 140 mL Kel-F chamber with an external syringe as a mercury reservoir to control the height of the drop. The chamber was filled with 1 mmol/L KCl aqueous solution which was deoxygenated by bubbling purified N_2 for 20−30 min. A thin mica sheet, glued to the lower surface of a horizontal glass disk, could be driven down toward the mercury surface with subnanometer control of its position. The back of the mica was half-silvered, enhancing optical interference between reflected rays from the silver and mercury surfaces, which was used to measure the distance between the mercury and the mica surface, i.e., the aqueous film thickness, with an accuracy of $\pm$0.5 nm or better.[43,46] The interferometric method was also used to measure the shape of the mercury drop, which enabled (a) calculation of the Laplace pressure from measurements of the drop curvature when the mica was far removed from it, and (b) drop flattening to be observed when the mica was pressed down toward it.

For repulsive surface forces operating between the mercury and mica the drop flattens if the mica is pressed down, so that a wetting film of the aqueous phase forms. The film has a uniform thickness, determined by the balance of disjoining pressure (associated with the surface force between mercury and mica) and the drop's internal pressure. The internal pressure is equal to the Laplace pressure across the protruding drop's curved surface before the mica is brought close to it. The disjoining pressure is created as a result of the surface charges on the mica and the mercury surfaces, with the latter controllable by applying a potential between the mercury and the aqueous phase. The data to be presented below are in the form of aqueous film thickness measurements as a function of the applied potential. Thus the measurements show how the film thickness changes at constant disjoining pressure (since the drop's internal pressure remains constant) if the mercury surface charge is varied. The film thickness depends on the potential at the outer Helmholtz plane (OHP) of the mercury (plus adsorbed layer)/water interface.[46]

An electric potential was applied to the mercury using a three-electrode system controlled by a potentiostat (Autolab PGSTAT-30, The Netherlands). A tube made from platinum gauze was placed symmetrically around the mercury capillary to act as a counter electrode; a saturated calomel electrode (SCE) was used as a reference electrode and the mercury was connected as the working electrode through a platinum wire. The potentiostat was also used to conduct cyclic voltammetry (CV) measurements during each experiment to confirm thiol deposition. Two types of CV measurement on thiol-decorated mercury were made: (a) in situ, with the mercury drop in its place for SFA measurements and the CV measurements made immediately after the film thickness measurements, and (b) ex situ measure-

ments made in separate experiments with a mercury drop in the same chamber filled with appropriate aqueous electrolyte solutions, but without the mica surface being present.

In SFA experiments surface cleanliness is of paramount importance, and experience shows that once a surface has been wet it should not be allowed to dry, in case unwanted solutes deposit on the surface. For this reason it was prudent to find an alternative self-assembly method to the usual procedure of depositing a thiol surfactant from organic solvent and then rinsing and/or drying the surface before transferring to aqueous solution for electrochemical measurements. The method we developed involves depositing the thiol in situ with the mercury already immersed in aqueous solution, using a small volume of ethanol which subsequently dissolves in a far greater volume of water. The appropriate thiol compound was dissolved in ethanol at a concentration of 10 mmol/L. With a mercury drop protruding from the capillary in the SFA chamber and the chamber filled with 140 mL of the background KCl solution, a 0.2 mL drop of the ethanolic thiol solution was injected very close to the mercury drop, using a Hamilton gastight syringe with a 22 gauge stainless steel needle inserted into the chamber through a rubber septum. This corresponds to a concentration of 13 μmol/L thiol in the whole aqueous chamber, but of course the concentration close to the mercury surface during deposition was much higher, probably by 2 or 3 orders of magnitude. No potential was applied to the mercury during thiol deposition, so it had its open-circuit potential (OCP) which we measured as -150 mV SCE before adding the thiol. On addition of thiol, the OCP was observed to decrease over several minutes, reequilibrating at -210 mV after about 10 min. At least 15 min[32] was allowed before measurements commenced. The mercury drop remained shiny and the optical interference fringes remained smooth after the deposition of each of the three thiol compounds.

The same apparatus (Figure 1) was used for drop profile measurements to measure the mercury/water interfacial tension. A video camera with a macro lens was used to record the image of the drop profile through a side window in the apparatus. The image was then analyzed using an axisymmetric drop shape analysis (ADSA) program "goccio" written by Busoni and Carlà,[49] which determines the interfacial tension γ from the shape and size of the drop. A ball bearing 3.000 ± 0.005 mm in diameter was used to calibrate magnification and check for distortion of the image. The interfacial tension was measured as a function of applied potential, and the resulting plot is the so-called electrocapillary curve.

The procedure for the interfacial tension measurements was as follows. The bare mercury curve was measured first and then thiol was deposited according to the method described above. After allowing time for open-circuit assembly of the monolayer to occur, a potential of 0 mV was applied and then decreased in 100 mV steps to -1600 mV, with the drop shape recorded after each step. The potential was returned to 0 mV and then increased to $+400$ mV in 100 mV steps for the final few measurements.

Presoftened water was purified with a Liquipure RO polishing system (Modulab XLCRO 1202, Continental, USA) and then distilled with an all-quartz subboiling distillation apparatus (Quartz et Silice, France). The background electrolyte used in all experiments was 1 mmol/L KCl, deoxygenated by purging with nitrogen as described above. KCl was purchased from Aldrich (BDH, Analytic Reagent Grade) and mixed with distilled water to prepare the electrolyte. The solution was unbuffered. This is normal procedure for SFA experiments, in order to keep the electrolyte species as simple as possible and also, in the present case, to maintain a low ionic strength. The aqueous film thicknesses measured below depend on the solution's Debye length, and it is convenient to have a large Debye length ($\sim$10 nm) which keeps the film thicknesses in the range of tens of nanometers. Mercury was purchased from Aldrich (electronic grade, 99.9999%), washed with dilute nitric acid, purged with high purity oxygen, and then rinsed copiously with purified water until all residual acid was removed.[43] Ethanol (Analytic Reagent, Univar) was used to make up thiol solutions. Mercaptoacetic acid ($HSCH_2COOH$) (97+%), 11-mercapto-1-undecanoic acid ($HS(CH_2)_{10}COOH$) (95%), 11-mercapto-1-undecanol ($HS(CH_2)_{10}CH_2OH$) (97%), 1-undecanethiol ($HS(CH_2)_{10}CH_3$) (98%), and $Ru(NH_3)_6Cl_3$ (98%) were purchased from Sigma-Aldrich and used without further treatment. All solution preparation, apparatus cleaning, and assembly operations were carried out in a class 3500 clean room.

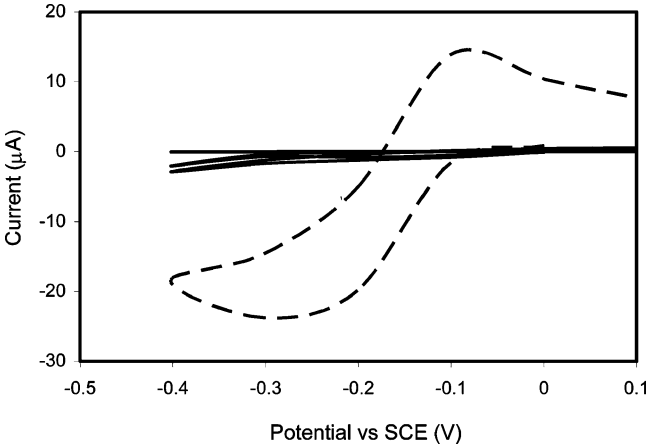

Figure 2. Ex situ cyclic voltammograms of mercury in a solution of 1 mmol/L $Ru(NH_3)_6Cl_3$ plus 1 mmol/L KCl, before (dashed line) and after (solid lines, three different experiments) deposition of 1-undecanethiol from ethanol at a final concentration of 13 μmol/L. Scan rate: 0.1 V/s.

3. Results

3.1. Monolayer Integrity. In order to confirm that our deposition procedure results in the formation of a monolayer that is compact and reasonably free of pinholes, a test similar to that used by Demoz and Harrison[31] was conducted. This involved measuring the CV of a redox active probe, $Ru(NH_3)_6^{2+/3+}$, at the mercury electrode before and after deposition of thiol. The potential range was limited to between $+0.1$ and -0.3 V to avoid reductive desorption of the thiol layer (to be described in section 3.3). Results for 1-undecanethiol are shown in Figure 2. It is clear that the presence of the thiol layer on the mercury surface is very effective at blocking the redox reaction, which demonstrates that a high-integrity monolayer has been formed. This measurement was repeated several times with new drops and new monolayer assemblies to verify that our deposition procedure works consistently well (three separate measurements are shown in Figure 2).

3.2. Electrocapillary Curves. The electrocapillary curve, i.e., the variation of the mercury/aqueous electrolyte interfacial energy γ with potential applied to the mercury, E, is shown in Figure 3 for bare mercury and mercury modified with two different thiol SAMs: 11-mercapto-1-undecanol and 1-undecanethiol. The mercury data show the familiar shape that is approximately an inverted parabola.[50−52] The maximum interfacial tension that we measure, 420 mJ/m^2, differs slightly from

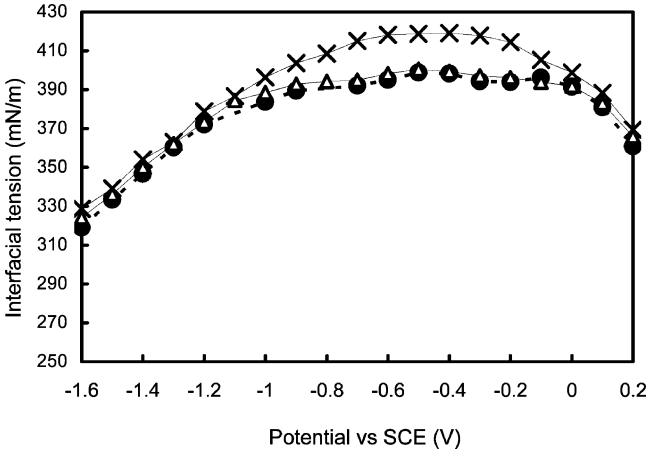

Figure 3. Electrocapillary curves of 11-mercapto-1-undecanol and 1-undecanethiol modified mercury in 1 mmol/L KCl. Crosses, bare mercury; empty triangles, 13 μmol/L 1-undecanethiol modified mercury; filled circles, 13 μmol/L 11-mercapto-1-undecanol modified mercury. Lines are included only to guide the eyes.

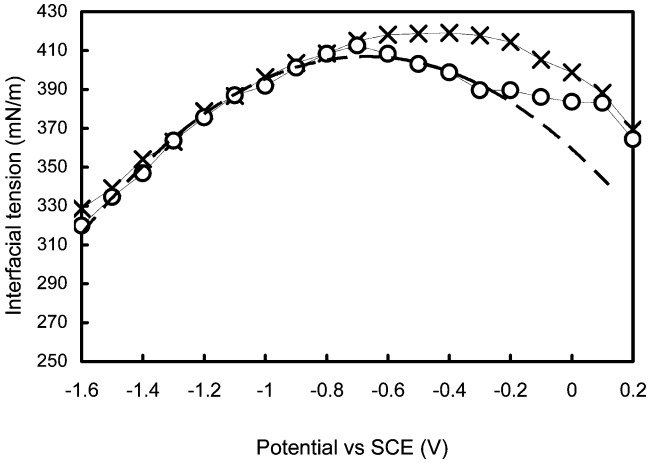

Figure 4. Electrocapillary curves of 11-mercapto-1-undecanoic acid modified mercury in 1 mmol/L KCl. Crosses, bare mercury; empty circles, 13 μmol/L 11-mercapto-1-undecanoic acid modified mercury; dashed line, fitted parabola, indicating the shift of the cathodic branch.

the accepted literature value of 427 mJ/m^2.[53] The difference is attributable to insufficient accuracy in the calibration of our optical imaging system, which introduces a systematic error to the data.[49] We are less concerned here, however, with absolute values than with relative changes in interfacial tension associated with adsorption of the thiol molecules.

The Lippmann equation

$$\sigma = -\frac{\partial \gamma}{\partial E}$$

relates the mercury surface charge σ to the negative gradient of the electrocapillary curve $\gamma(E)$. We note, for later discussion, that in the presence of a charged adsorbate the mercury surface charge can differ in sign from the potential at the outer Helmholtz plane. From this, it is seen that the bare mercury surface is negatively charged if the applied potential is more negative than about -400 mV with respect to the saturated calomel electrode (SCE), and positively charged if the applied potential is above that value. The maximum at approximately -400 mV SCE marks the point of zero charge (PZC).

In the presence of thiols the interfacial tension of mercury is reduced in the neighborhood of the PZC, giving clear evidence for adsorption, and the behavior of these two thiols is the same within our experimental accuracy. Between approximately -1100 and 0 mV the curve is fairly flat, indicating a low surface charge on the mercury. The position of the PZC does not appear to have shifted significantly, although the curve is so flat that it is difficult to locate the PZC precisely. Outside this range of potential the interfacial tension is the same (within experimental error) as that measured on a bare mercury drop.

Such behavior is similar to what has previously been reported[54] for a system where medium-chain alcohols in aqueous solution adsorb to a mercury surface and the electrocapillary curve shows a plateau within a certain potential range. Recently, Busoni[55] measured the electrocapillary curve of dioleylphosphatidylcholine (DOPC) lipid films on mercury in aqueous solution and showed that the interfacial tension is decreased by 50 mN/m at the PZC by the DOPC film and remains constant between 0 and -1100 mV. This is in good agreement with our results; however, the different adsorbates used here result in a smaller decrease (30 mN/m) of the interfacial tension. The constant interfacial tension implies a stable and densely packed monolayer formed at the interface. When the electrode is highly polarized (positive enough or negative enough), the SAM is desorbed and the interfacial tension is equal to that measured on a bare mercury surface.

The similarity of the electrocapillary curves for mercury modified by the two compounds 1-undecanethiol and 11-mercapto-1-undecanol, and in particular the fact that they are desorbed at about the same potentials, supports the notion that the bonding of each thiol to mercury is similar. Since there is little doubt that the alkanethiol is attached via its terminal thiol group, this suggests that the mercapto alcohol also bonds via its thiol terminus and not via its hydroxyl end. We note also that mercaptohexanol is known to adsorb to gold via its thiol end, and this molecule is commonly used as a blocking agent for protein adsorption in experiments with SAMs on gold, because the hydroxyl at the upper end of the mercaptohexanol layer is hydrated and resists protein attachment.[56,57]

If 11-mecaptoundecanoic acid is adsorbed at the same concentration, the electrocapillary curve differs from those for the two uncharged thiols, as shown in Figure 4. As the potential is decreased from 0 to -300 mV the interfacial tension in this case increases only slightly, similar to the behavior of the two uncharged thiols described above. However between -300 and -700 mV γ increases more rapidly, reaching a distinct maximum near -700 mV. At potentials below that the data follow the curve for bare mercury.

The dashed line in Figure 4 shows that part of the data follows approximately an inverse parabolic curve, which describes the bare mercury curve at negative potentials but reaches a maximum (PZC) at lower potential and falls below the mercury curve at more positive potentials. This behavior is well-known for electrolyte systems in which specific anion adsorption occurs;[58] for example, the cathodic branch of the electrocapillary curve of mercury in NaI electrolyte is shifted negatively compared to the one measured in NaF electrolyte because I^- adsorbs more strongly than F^- does. In the present experiment, adsorption of the thiol brings charged COO^- groups to the surface.

3.3. Cyclic Voltammograms. The cyclic voltammograms (CVs) for a mercury drop with 11-mercapto-1-undecanoic acid deposited at various concentrations, measured ex situ, are shown in Figure 5. For a concentration of 6.7 μmol/L (in the whole chamber) the CV curve is featureless, similar to that of the bare mercury drop. However, if the concentration is 13 μmol/L or greater, the CV is distinctly different, indicating that at this

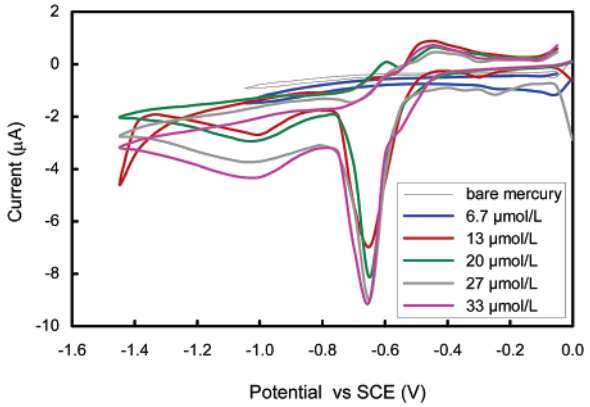

Figure 5. Ex situ CVs of 11-mercapto-1-undecanoic acid modified mercury in 1 mmol/L KCl solution for various thiol concentrations indicated in the legend. Scan rate: 0.05 V/s.

concentration the presence of the thiol has modified the mercury surface. The main feature is a desorption peak at around −650 mV SCE, with a weak readsorption peak near −450 mV when the potential is increased again. The desorption peaks are attributed to the reduction of the thiol−mercury complex on the mercury:[32]

$$\mathrm{Hg(SR)}_{y(\mathrm{ads})} + y\mathrm{H}^+ + y\mathrm{e}^- \rightarrow y\mathrm{RSH} + \mathrm{Hg}$$

With increasing thiol concentrations (20, 27, and 33 μmol/L), the desorption peak is observed at the same potential with comparable peak areas. Assuming the diameter of the mercury drop is equal to the size of the capillary tube (3 mm) and the drop shape is a hemisphere, the surface area of the mercury is 0.14 cm^2. The peak area at 13 μmol/L gives an estimate of (95 ± 10) μC/cm^2, which agrees with previous measurements[35] for densely packed thiol monolayers on mercury. This corresponds to (17 ± 2) Å^2/molecule (note that the area is unlikely to be less than the cross-sectional area per alkane chain in a crystal, 18.3 Å^2) or (9.9 ± 1.0) × 10^{-10} mol/cm^2, which is a more dense packing than is typical for a thiol SAM on gold (7.8 × 10^{-10} mol/cm^2). The difference is consistent with perpendicular orientation of alkane chains of thiols on mercury compared to their 30° tilt on gold.[33,34] There is also a broad, shallow cathodic peak observed at −1000 mV. This can be attributed to desorption of physisorbed thiol molecules, as suggested by Muskal and Mandler.[14]

Because a concentration of 13 μmol/L is the minimum required to show evidence of an adsorbed layer, and the main features of the CV do not change significantly at higher concentrations, this was the concentration used for all other studies on the thiol-modified mercury.

The CV for this thiol layer was also measured in situ, i.e., with a mica surface close to the mercury drop (Figure 6). This measurement was made at the end of a series of SFA measurements that are described below. Qualitatively the curve has the same features, a desorption peak near −600 mV and an adsorption peak near −400 mV. The peaks are shifted slightly from those in the CV measured ex situ, and the desorption peak is broader. The difference may be due to the different history of the thiol layer (which will be discussed in more detail below), or it may be due to the different geometry of the electrochemical cell, with the proximity of the mica surface to the mercury drop working electrode affecting the cell impedance and probably hindering the diffusion of species to and from the mercury surface.

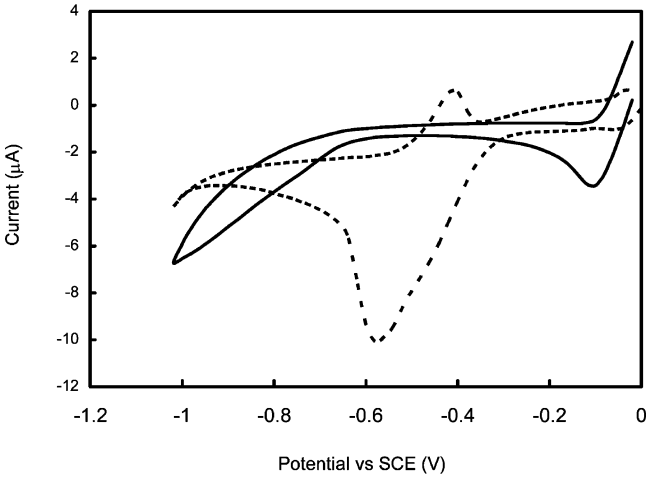

Figure 6. In situ cyclic voltammogram of 13 μmol/L 11-mercapto-1-undecanoic acid modified mercury in 1 mmol/L KCl electrolyte measured in the SFA with a mica surface close to the mercury drop. Solid line, bare mercury; dashed line, thiol-modified mercury.

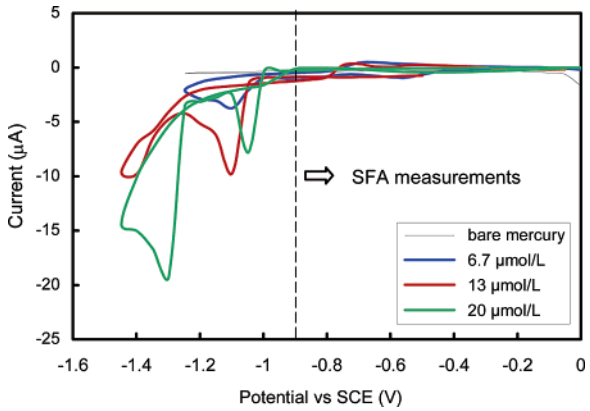

Figure 7. Cyclic voltammograms of 11-mercapto-1-undecanol modified mercury measured ex situ in 1 mmol/L KCl solution for various thiol concentrations indicated in the legend. Scan rate: 0.05 V/s.

The cyclic voltammograms measured ex situ for 11-mercapto-1-undecanol at three concentrations are shown in Figure 7. These show two cathodic peaks, the first at −1 to −1.1 V SCE, and the second at −1.3 to −1.4 V, the position depending on thiol concentration. The first peak is attributed to reductive desorption, as before. It has shifted to a more negative potential compared to the carboxylic acid thiol CVs shown in Figure 5. The difference in desorption energy may be due to the higher electrostatic energy due to repulsion between charged headgroups in the carboxylic acid SAM (further evidence of this is given in the following section), and the different solubilities of these two thiols in water may also be a factor. The positions of the desorption peaks for the anionic and neutral thiols is also consistent with the potentials at which their electrocapillary curves join up with the bare mercury curves (Figures 3 and 4), at around −700 mV (carboxylic acid) and −1100 mV (undecanol), respectively.

The mercaptoundecanol CV at the lowest concentration, 6.7 μmol/L, shows only a weak desorption peak at −1.1 V. The weak peak indicates that little thiol was desorbed, probably because only a small amount had been adsorbed in the first place at this concentration, as previously noted for the carboxylic acid thiol (see Figure 5). At 13 μmol/L the desorption peak area gives 10.6 × 10^{-10} mol/cm^2, comparable to what was measured for the dense monolayer formed by mercaptoundecanoic acid. Hence this concentration was used for the SFA

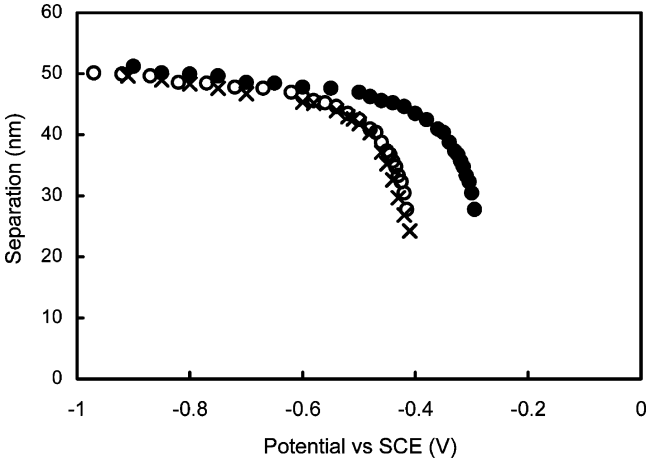

Figure 8. Variation of film thickness between 13 μmol/L 11-mercapto-1-undecanol modified mercury drop with an internal (Laplace) pressure of 560 Pa, and a mica surface in 1 mmol/L KCl solution. Crosses, bare mercury; filled circles, SAM-modified mercury; open circles, SAM-modified mercury data shifted by −120 mV in potential.

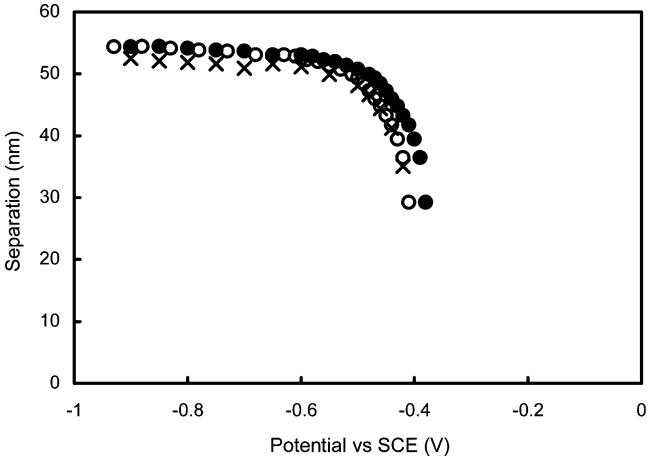

Figure 9. Variation of film thickness between 13 μmol/L 1-undecanethiol modified mercury drop with an internal pressure of 473 Pa, and a mica surface in 1 mmol/L KCl solution. Crosses, bare mercury; filled circles, modified mercury; open circles, modified mercury with a shift of −30 mV in potential.

experiments described below. For all of the thiol concentrations, there is no noticeable readsorption peak observed for the mercaptoundecanol.

All of the SFA data for this thiol were measured at potentials more positive than −900 mV, so from the CV no desorption phenomena would be expected in this range. The CV for 1-undecanethiol was not measured (apart from the data over a small potential range in the presence of $Ru(NH_3)_6^{2+/3+}$ shown in Figure 2).

3.4. Film Thickness Measurements To Probe OHP Potential. As described in the Introduction, previous measurements of the aqueous film thickness between a mica surface and a flattened mercury drop have been analyzed in terms of the electrical double-layer forces acting between the mica and the mercury surfaces. The film thickness at which the drop flattens is the drop−solid surface separation at which the disjoining pressure due to double-layer forces equals the Laplace pressure of the drop, which is calculated from a measurement of the drop's curvature before it is flattened.[46] Typical values for the millimeter-scale drops used in our experiments are about 500 Pa. (Note that van der Waals forces are negligible at the film thicknesses of tens of nanometers reported here and previously.) The data can be compared with well-established theories of double-layer interactions to find the value of surface potential at the mercury/aqueous interface from the known surface potential of mica and the film thickness. The double-layer interaction depends on the diffuse layer or outer Helmholtz plane (OHP) potential at the outermost point of any adsorbed layer on the mercury.

Figure 8 shows the results of film thickness measurements to determine the effect of an adsorbed layer of 11-mercapto-1-undecanol on the OHP potential. Two data sets are shown: the first is for bare mercury (crosses), which is a repeat measurement similar to the previously published data from our group.[46] This shows that a stable aqueous film exists between mercury and mica if a sufficiently large negative potential is applied to the mercury phase. If the potential is gradually increased (i.e., made less negative), the film becomes thinner, and collapses at a potential close to the PZC. A detailed discussion of this behavior is given in ref 46. At potentials above the PZC the mercury surface is positively charged, so it is attracted toward the mica and the aqueous film becomes unstable. The second data set (filled circles) in Figure 8 shows similar behavior, except that the entire curve appears to be shifted to higher (more positive) potentials. To show that the shift is uniform, the same data are replotted with a constant shift of 120 mV to the left (open circles), and they overlay the bare mercury data very closely.

From a comparison with the standard Gouy−Chapman theory of double-layer interactions, Connor and Horn[46] showed that the bare mercury data can be fitted accurately by assuming the OHP potential of mercury to be equal to the applied potential (measured with respect to SCE) shifted by a constant that is close to, but not quite the same as, the PZC. The present data suggest that, with the adsorbed thiol layer, the OHP potential is also simply shifted from the applied potential, but now with a different shift. We will return to this point in the Discussion.

Figure 9 shows a comparable set of measurements for a mercury drop before (repeated) and after deposition of a layer of 1-undecanethiol. Similar to the results shown in Figure 8, the effect of the alkanethiol layer is simply to introduce a constant horizontal shift in the data, that is, to change the constant difference between OHP and applied potential measured with respect to SCE. The shift in this case is +30 mV, which differs by 90 mV from the shift determined earlier (+120 mV) for the hydroxy-terminated thiol of the same chain length.

Film thickness data for mercury modified by 11-mercapto-1-undecanoic acid are qualitatively different, as shown in Figure 10. After depositing the thiol at the OCP, i.e., with no potential applied to the mercury, a large negative potential was applied and the mica brought toward the drop until the latter was flattened. The potential was then made more positive. In contrast to the bare mercury behavior, a stable aqueous film remained between the carboxylic acid thiol-modified mercury and the mica surface if the potential was increased all the way to 0 mV SCE. Evidently, with 11-mercapto-1-undecanoic acid adsorbed to the mercury, some or all of the carboxylic acid groups have dissociated at the pH of the solution (1 mmol/L KCl, pH 6.2) and a net negative charge resides within the outer Helmholtz plane. Without the thiol, mercury is positively charged at zero applied potential.

Several potential scans were made from 0 mV to a negative value and then returned to zero again. With the first two scans, to −750 mV and then to −900 mV, there was a slight decrease (about 10 nm) in film thickness on reducing the potential, and a fairly constant film thickness as the potential was returned to

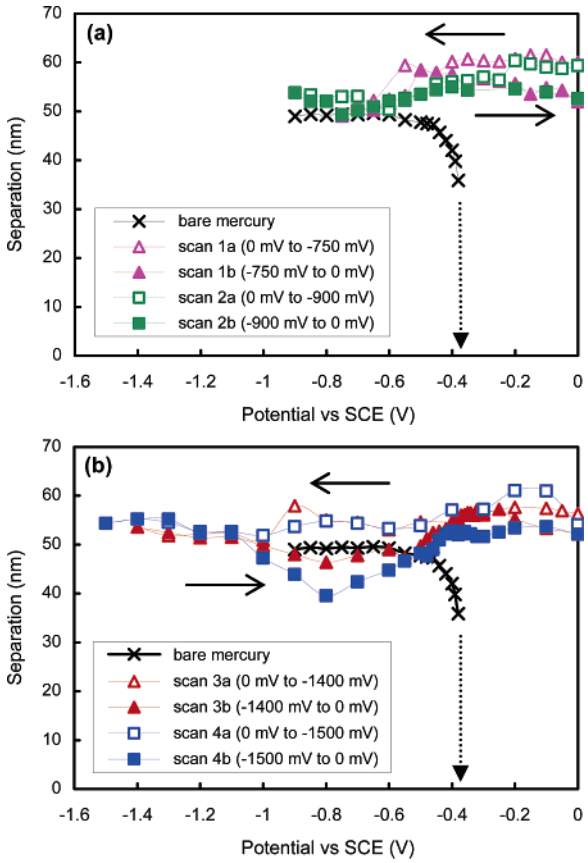

Figure 10. Variation of film thickness between 13 μmol/L 11-mercapto-1-undecanoic acid modified mercury drop and a mica surface in 1 mmol/L KCl solution. (a) Black crosses, bare mercury; magenta triangles, modified mercury, scan 1 (empty triangles, negative scan; filled triangles, positive scan); green squares, modified mercury, scan 2 (empty squares, negative scan; filled squares, positive scan). (b) Black crosses, bare mercury; Red triangles, modified mercury, scan 3 (empty triangles, negative scan; filled triangles, positive scan); blue squares, modified mercury, scan 4 (empty squares, negative scan; filled squares, positive scan).

0 mV. At the end of each scan, the film thickness increased by 5−10 nm over a period of about 10 min while holding the potential at 0 mV before commencing the next scan. The third and fourth scans were taken to larger negative potentials, −1400 and −1600 mV, respectively. In both cases the film thickness decreased slightly as the potential was reduced to the end of the scan. On increasing the potential again, the film thickness decreased further in the neighborhood of −800 mV, and then increased again between −800 and 0 mV. The thickness of the film at its minimum decreased with each successive scan.

Two other thiol depositions were investigated by film thickness measurements in the SFA (results not shown). In one, 11-mercapto-1-undecanoic acid was deposited at a lower concentration (0.67 μmol/L compared to 13 μmol/L). The behavior with this SAM was initially similar to the SAM formed from the higher concentration (Figure 10), insofar as a stable aqueous film was observed between the mica and the modified mercury surface at zero applied potential. Several potential scans to more negative numbers were performed, and the film remained stable after scanning to −1100 mV. However, after scanning the potential to −1400 mV, the drop behaved like bare mercury and the film collapsed near the PZC when the potential was increased again. This indicates that most or all of the SAM had been removed by scanning to a sufficiently negative potential. Thus it is not impossible to remove the SAMs formed by a longer chain length thiol if a lower thiol concentration is used.

The second alternative thiol deposition involved a very short chain thiol (mercaptoacetic acid) which was deposited according to the same method. Initially the behavior was the same: a stable aqueous film was observed at 0 mV, indicating the presence of a negatively charged thiol layer on the mercury. However, the thiol was easily desorbed by scanning the potential to −750 mV, as evidenced by the fact that the variation of film thickness was similar to that with the bare mercury drop, collapsing near the PZC when the potential was increased again.

4. Discussion

The three sets of data, namely electrocapillarity (EC), cyclic voltammetry (CV), and film thickness measurements, all present a consistent picture of adsorption of thiols to mercury. The behavior of the two uncharged thiols, terminated by $-CH_3$ and −OH, respectively, is quite similar, with evidence from EC and CV of adsorption to mercury for applied potentials between −1100 and 0 mV. The similarity in desorption potentials gives reason to believe that both molecules are adsorbed to mercury via their terminal thiol groups. Each of these thiols produces a constant shift of the OHP potential at the mercury/water interface (which will be discussed in more detail later).

The −COOH terminated thiol also adsorbs to mercury around the PZC, as evidenced by the EC and CV curves. Reductive desorption in this case begins to occur if the potential is reduced to between −600 and −700 mV. The CV suggests that desorption is not complete in that region, with further effects occurring around −1100 mV. However, the EC curve shows that below −700 mV there is very little change to the mercury/water interfacial tension.

The 11-mercaptoundecanoic acid SAM is more robust (keeping a higher surface charge density) and is more difficult to desorb than the short-chain thiol (mercaptoacetic acid). This can be attributed to hydrophobic interactions and interchain attractions that favor the formation and stabilization of a densely packed SAM for the higher homologue.

The effect of the carboxylic acid thiol SAM on the film thickness is qualitatively different from that of the two uncharged thiols. The presence of this thiol on the mercury surface creates a repulsive force against the negatively charged mica, even in a potential range (−400 to 0 mV) at which the underlying mercury surface is positively charged, as seen from the electrocapillary data of Figure 3. Evidently some of the COOH groups have dissociated to form COO^- groups on the surface, at a sufficiently high density to overcompensate the mercury's positive charge. From an estimate of the electrocapillary curve gradient in the vicinity of −400 mV and the Lippman equation, the mercury charge is around +0.06 C/m^2, i.e., 6 μC/cm^2. This corresponds approximately to one charge for every 16 molecules adsorbed in the SAM, so at least this fraction of the adsorbed molecules in the SAM must be negatively charged to outweigh the mercury charge and create the repulsive double-layer force.

The pK_a of long-chain carboxylic acid thiol SAMs formed on rough gold surfaces is around 5−6, and it is thought to be as much as 3 pH units higher for SAMs formed on smooth surfaces.[59] Nevertheless, titration curves appear rather broad, covering several pH units, for carboxylic acid in a SAM[60] so that partial dissociation is possible at pH a few units below the pK_a. Our experimental pH was 6.2. It should be borne in mind that pH in the neighborhood of a charged surface may be

significantly different from that far from the surface, changing by one unit for every 25 mV (approximately) in local potential. Thus, on the anodic side of the mercury PZC the local pH may be up to several units higher, facilitating the dissociation of the carboxylic acid group. Conversely, on the cathodic side the pH close to the surface would be lower, and in this region the carboxylic acid is unlikely to be dissociated. However, it remains adsorbed in its neutral form, and the mercury is negatively charged in this region. Hence the total charge inside the outer Helmholtz plane can be negative on both sides of the PZC, consistent with our observation of repulsion against mica at all applied potentials between 0 and −1.5 V SCE.

While the qualitative film thickness is simple to explain, the detailed behavior is not so straightforward. From Figure 10 it is seen that the film thickness between the −COOH thiol decorated mercury and mica is as much as 15 nm greater than that with bare mercury. At an applied potential of −900 mV the OHP potential is effectively "infinite" in magnitude, in the sense that the double-layer repulsion with mica is saturated, and any further increase in the magnitude of the OHP potential does not increase the film thickness beyond about 52 nm at the experimental electrolyte concentration.[46] A film thickness greater than this cannot be explained simply by an increase in surface charge on the mercury.

Possible explanations for the thicker film (up to 63 nm) observed with the COOH thiol present are as follows:

1. The OHP, i.e., the plane at which the outermost surface charges reside, has moved out from the mercury surface toward the electrolyte solution. Note that the optical interference method measures the thickness between the mica surface and the reflective mercury interface (changes in refractive index due to adsorbed thiol surfactant produce a negligible error in the calculation of thickness from the measured interference wavelengths). An adsorbed layer of charged thiol molecules is likely to shift the OHP away from the mercury surface, but a single monolayer of 11-mercapto-1-undecanoic acid could only account for a shift of about 1 nm.

2. Adsorption of carboxylic acid thiol to mica would (a) shift the OHP and (b) increase the negative surface charge at that interface. However, anionic surfactants in general do not adsorb to mica (which is negatively charged), so we do not favor this explanation.

3. The film thickness is measured at the mica−mercury separation where disjoining pressure is equal to the internal Laplace pressure of the mercury drop. Since the adsorption of thiols reduces the mercury/electrolyte interfacial tension, the Laplace pressure of the drop could be reduced, which means that it would be balanced by a lower disjoining pressure at a greater film thickness. However, the Laplace pressure of the drop is calculated from the drop curvature measured after the thiol layer has been adsorbed. We have made detailed calculations of drop deformation based on the Young−Laplace equation augmented by including the effects of disjoining pressure. The calculation shows that the maximum change in Laplace pressure would be less than 10% if the thiol layer on a mercury drop were to desorb fully during its interaction with mica. Double-layer disjoining pressure calculations show that this would cause only about 0.5 nm change in film thickness, which is not enough to account for the observed change.

4. The thickness change could be accounted for if more than a single monolayer of carboxylic acid thiol adsorbed to mercury, shifting the OHP out by more than a single molecular length (see (1) above) and/or introducing steric repulsion corresponding to the adsorbed layer thickness. However, according to Muskal and Mandler,[36] multilayer adsorption on mercury only occurs for thiols with short alkane chain lengths, so it is an unlikely explanation for the present observations.

5. A significant feature of the observed film thickness is that it increases by ∼10 nm over a period of 10 min while the potential is held at 0 mV, indicating some transient behavior. It has been observed by one of us[61] that partial desorption of a thiol layer on mercury can cause a temporary increase in local solute concentration and osmotic pressure of the aqueous film between a flattened mercury drop and mica, because the desorbed molecules are slow to diffuse out of the gap (which is ∼50 nm thick and ∼100 μm in extent). The diffusion takes ∼30 min,[61] during which time the transient enhancement of osmotic pressure acts like an additional contribution to disjoining pressure, pushing the mercury away from the mica surface. The observation of film thickness increasing while the potential is held constant is consistent with this explanation. Another reason for this type of transient behavior due to concentration gradients has been suggested by a reviewer, who noted that any change in the state of ionization in the carboxylic acid monolayer would result in a significant pH shift in the (unbuffered) thin film between the mercury and mica, and slow diffusion of protons in or out of the thin film would give similar time-dependent effects.

Of these possibilities, only the last one (5) is able to account for the observed thickness increase of more than 10 nm. This slow dynamic effect coupled with possible desorption or adsorption of the thiol molecules or association/dissociation of their acid groups means that the film thickness is likely to be history-dependent, which should be kept in mind when designing an experimental protocol.

We now return to discuss the film thickness behavior observed if SAMs are formed from the two uncharged thiols, 11-mercaptoundecanol and 1-undecanethiol. Each appears to introduce a (different) constant shift in the OHP for a given value of potential applied between the mercury and electrolyte phases (Figures 8 and 9). Since neither of these adsorbates is charged, the shift in OHP must be attributed to other effects. One is that thiol adsorption displaces a small amount of charge arising from Cl^- adsorption from the background electrolyte, which according to previous measurements in our laboratory increases the OHP by about 25 mV (i.e., makes it less negative for a given applied potential). This is not enough to account for the observed shift (a decrease) in the OHP of (120 ± 10) mV if the 11-mercaptoundecanol is adsorbed. The other effect that can account for this shift is a change in the so-called dipole potential of the mercury/electrolyte interface.

Dipole potential is the difference between Galvani potentials of adjacent phases, in this case mercury and the aqueous electrolyte. It originates in the inhomogeneity of the electron distribution perpendicular to the interface on the mercury side due to the existence of a phase boundary, and in a net dipole moment due to preferred orientation of water molecules adjacent to the mercury surface. Both parts would be affected by adsorption of a thiol layer (or any other adsorbate): the electronic distribution in the mercury will be affected by changing its neighbors across the interface (particularly if chemical bonding is involved), and adsorption will displace water molecules from the mercury surface and move them to a greater separation. There, at the outer edge of the SAM, their orientation will depend on the chemical nature of the distal end of the thiol molecule.

Trasatti[63] has listed some estimations of the change in dipole potential of water on mercury, based on the shift in potential

of zero charge caused by the adsorption of organic molecules on mercury. Changes in dipole potential were reported from 70 to 240 mV, depending on the type of organic molecule used and the coverage of these molecules. The changes in dipole potential measured here are of comparable magnitude.

The combined effect on dipole potential if a SAM of 11-mercapto-1-undecanol forms is a change of (120 ± 10) mV. It is not possible from this single value to separate the effects of the electron distribution and water dipole orientation components. However, a similar measurement made in the presence of a SAM of similar chemistry and molecular length, 1-undecanethiol, gives a smaller change from the bare mercury: (30 ± 10) mV in the same direction. Since the only difference between the SAMs is in the chemical moiety at the distal end of the adsorbate molecules, it is reasonable to suppose that the electron distribution in mercury should be very similar between these two cases. Therefore the difference between the two shifts in dipole potential, (90 ± 20) mV, is attributable to the change in water molecule orientation at the outer edge of the two SAMs, terminated by −OH and $-CH_3$ groups, respectively. The OHP is more negative at the hydrophobic $-CH_3$ surface than at the hydrophilic −OH one. The details of water dipole orientation, hydrogen bonding, and possible preferential adsorption of ions at these surfaces that would account for this difference may also be related to the observed fact that OHP potentials at oil−water and air−water interfaces are negative.

5. Concluding Remarks

Three different SAMs formed on mercury by thiol molecules of the same C_{10} chain length but different terminal groups have been investigated in the fluid-drop SFA. Complementary measurements of electrocapillary curves, cyclic voltammograms, and film thickness vs applied potential data at constant drop pressure were made. There is clear evidence for a net negative charge at the surface of a carboxylic acid terminated thiol SAM, although quantitative determination of the charge (or OHP potential) from double-layer pressure measurements was hampered by nonequilibrium and history-dependent effects.

SAMs formed from methyl-terminated and hydroxy-terminated thiols are nominally uncharged, but they have a clear and quantifiable effect on the dipole potential of the mercury/water interface. The difference between the dipole potentials with these two SAMs allows for an evaluation of the effects on dipole potential of water structure at hydrophobic $-CH_3$ and hydrophilic −OH surfaces.

In the future the mercury−SFA technique could be used to explore the comportment and surface chemistry of more complex SAMs formed on mercury. For example, measurements of film thickness between mica and mercury decorated by SAMs incorporating lipids or other biological molecules could be used to explore the interactions of those molecules in a realistic (fluid and laterally mobile) biomimetic membrane.

Acknowledgment. The authors thank Marcello Carlà and Lorenzo Busoni for graciously allowing us to use their axisymmetric drop shape analysis program "goccio", Rob Jones for helping us to set it up, Satomi Onishi for assistance with some of the experiments, Jason Connor and Helmuth Möhwald for helpful discussions, and Roland Benz for a critical reading of the manuscript. We are also grateful to the two reviewers of the original manuscript whose insightful comments have led to significant improvements. This work was funded by the Australian Research Council through the Special Research Centre for Particle and Material Interfaces. L.Y.C. gratefully acknowledges the Max-Planck-Gesellschaft for the award of an International Max Planck Research School scholarship.

References and Notes

(1) Laibinis, P. E.; Hickman, J. J.; Wrighton, M. S.; Whitesides, G. M. *Science* **1989**, *245*, 845.
(2) Bain, C. D.; Biebuyck, H. A.; Whitesides, G. M. *Langmuir* **1989**, *5*, 723.
(3) Bain, C. D.; Barry Troughton, E.; Tao, Y.-T.; Evall, J.; Whitesides, G. M. *J. Am. Chem. Soc.* **1989**, *111*, 321.
(4) Abbott, N. L.; Whitesides, G. M. *Langmuir* **1994**, *10*, 1493.
(5) Abbott, N. L.; Gorman, C. B.; Whitesides, G. M. *Langmuir* **1995**, *11*, 16.
(6) Ostuni, E.; Chapman, R. G.; Liang, M. N.; Meluleni, G.; Pier, G.; Ingber, D. E.; Whitesides, G. M. *Langmuir* **2001**, *17*, 6336.
(7) Holmlin, R. E.; Haag, R.; Chabinyc, M. L.; Ismagilov, R. F.; Cohen, A. E.; Terfort, A.; Rampi, M. A.; Whitesides, G. M. *J. Am. Chem. Soc.* **2001**, *123*, 5075.
(8) Becucci, L.; Moncelli, M. R.; Guidelli, R. *J. Electroanal. Chem.* **1996**, *413*, 187.
(9) Peggion, C.; Formaggio, F.; Toniolo, C.; Becucci, L.; Moncelli, M. R.; Guidelli, R. *Langmuir* **2001**, *17*, 6585.
(10) Becucci, L.; Moncelli, M. R.; Guidelli, R. *Langmuir* **2003**, *19*, 3386.
(11) Tamada, K.; Ishida, T.; Knoll, W.; Fukushima, H.; Colorado, R.; Graupe, M.; Shmakova, O. E.; Lee, T. R. *Langmuir* **2001**, *17*, 1913.
(12) Tamada, K.; Hara, M.; Sasabe, H.; Knoll, W. *Langmuir* **1997**, *13*, 1558.
(13) Textor, M.; Ruiz, L.; Hofer, R.; Rossi, A.; Feldman, K.; Hahner, G.; Spencer, N. D. *Langmuir* **2000**, *16*, 3257.
(14) Muskal, N.; Mandler, D. *Curr. Sep.* **2000**, *19*, 49.
(15) Ulman, A. *An introduction to ultrathin organic films: from Langmuir-Blodgett to self-assembly*; Academic Press: San Diego, 1991.
(16) Finklea, H. O. Self-assembled monolayers on electrodes. In *Encyclopedia of analytical chemistry*; Meyers, R. A., Ed.; John Wiley & Sons Ltd.: Chichester, U.K., 2000; p 1.
(17) Ederth, T.; Tamada, K.; Claesson, P. M.; Valiokas, R.; Colorado, R., Jr.; Graupe, M.; Shmakova, O. E.; Lee, T. R. *J. Colloid Interface Sci.* **2001**, *225*, 391.
(18) Evans, S. D.; Ulman, A. *Chem. Phys. Lett.* **1990**, *70*, 462.
(19) Fukushima, H.; Seki, S.; Nishikawa, T.; Takiguchi, H.; Tamada, K.; Abe, K.; Colorado, R., Jr.; Graupe, M.; Shmakova, O. E.; Lee, T. R. *J. Phys. Chem. B* **2000**, *104*, 7417.
(20) Ulman, A. *Thin Films: Self-assembled monolayer of thiols*; Academic Press: New York, 1998; Vol. 24.
(21) Zhao, X.-M.; Wilbur, J. L.; Whitesides, G. M. *Langmuir* **1996**, *12*, 3257.
(22) Nuzzo, R. G.; Allara, D. L. *J. Am. Chem. Soc.* **1983**, *105*, 4481.
(23) Laibinis, P. E.; Whitesides, G. M.; Allara, D. L.; Tao, Y.-T.; Parikh, A. N.; Nuzzo, R. G. *J. Am. Chem. Soc.* **1991**, *113*, 7152.
(24) Ulman, A. *J. Mater. Educ.* **1989**, *11*, 205.
(25) Levins, J. M.; Vanderlick, T. K. *Polym. Prepr. (Am. Chem. Soc., Div. Polym. Chem.)* **1991**, *32*, 216.
(26) Yamamoto, Y.; Nishihara, H.; Aramaki, K. *J. Electrochem. Soc.* **1993**, *140*, 436.
(27) Stewart, K. R.; Whitesides, G. M.; Godfried, H. P.; Silvera, I. F. *Surf. Sci.* **1986**, *57*, 1381.
(28) Hofer, R.; Textor, M.; Spencer, N. D. *Langmuir* **2001**, *17*, 4014.
(29) Brovelli, D.; Hahner, G.; Ruiz, L.; Hofer, R.; Kraus, G.; Waldner, A.; Schlösser, J.; Oroszlan, P.; Ehrat, M.; Spencer, N. D. *Langmuir* **1999**, *15*, 4324.
(30) Schonenberger, C.; Sondag-Huethorst, J. A. M.; Jorritsma, J.; Fokkink, L. G. J. *Langmuir* **1994**, *10*, 611.
(31) Demoz, A.; Harrison, D. J. *Langmuir* **1993**, *9*, 1046.
(32) Muskal, N.; Turyan, I.; Mandler, D. *J. Electroanal. Chem.* **1996**, *409*, 131.
(33) Deutsch, M.; Magnussen, O. M.; Ocko, B. M.; Regan, M. J.; Pershan, P. S. *Thin Films* **1998**, *24*, 179.
(34) Magnussen, O. M.; Ocko, B. M.; Deutsch, M.; Regan, M. J.; Pershan, P. S.; Abernathy, D.; Grubel, G.; Legrand, J. F. *Nature* **1996**, *384*, 250.
(35) Stevenson, K. J.; Mitchell, M.; White, H. S. *J. Phys. Chem. B* **1998**, *102*, 1235.
(36) Muskal, N.; Mandler, D. *Electrochim. Acta* **1999**, *45*, 537.
(37) Moncelli, M. R.; Becucci, L. *J. Electroanal. Chem.* **1997**, *433*, 91.
(38) Moncelli, M. R.; Becucci, L. *J. Electroanal. Chem.* **1995**, *385*, 183.
(39) Herrero, R.; Barriada, J. L.; Lopez-Fonsec, J. M.; Moncelli, M. R.; Sastre de Vicente, M. E. *Langmuir* **2000**, *16*, 5148.
(40) Buoninsegni, F. T.; Herrero, R.; Moncelli, M. R. *J. Electroanal. Chem.* **1998**, *452*, 33.
(41) Becucci, L.; Moncelli, M. R.; Herrero, R.; Guidelli, R. *Langmuir* **2000**, *16*, 7694.

(42) Haag, R.; Rampi, M. A.; Holmlin, R. E.; Whitesides, G. M. *J. Am. Chem. Soc.* **1999**, *121*, 7865.
(43) Connor, J. N. Measurement of Interactions between Solid and Fluid Surfaces: Deformability, Electrical Double Layer Forces and Thin Film Drainage. Ph.D. Thesis, University of South Australia, 2001.
(44) Connor, J. N.; Horn, R. G.; Miklavcic, S. J. *Uzbek J. Phys.* **1999**, *1*, 99.
(45) Connor, J. N.; Horn, R. G. *Rev. Sci. Instrum.* **2003**, *74*, 4601.
(46) Connor, J. N.; Horn, R. G. *Langmuir* **2001**, *17*, 7194.
(47) Connor, J. N.; Horn, R. G. *Faraday Discuss.* **2003**, *123*, 193.
(48) Clasohm, L. Y.; Connor, J. N.; Vinogradova, O. I.; Horn, R. G. *Langmuir* **2005**, *21*, 8243.
(49) Busoni, L.; Carla, M.; Lanzi, L. *Rev. Sci. Instrum.* **2001**, *72*, 2784.
(50) Bard, A. J.; Faulkner, L. R. *Electrochemical Methods: Fundamentals and Applications*; John Wiley & Sons: New York, 1976.
(51) Bockris, J. O. M.; Reddy, A. K. N. *Modern Electrochemistry*; Macdonald: London, 1970; Vol. 2.
(52) Bockris, J. O. M.; Khan, S. U. M. *Surface Electrochemistry: A Molecular Level Approach*; Plenum Press: New York, 1993.
(53) Conway, B. E. Properties of the Electric Double Layer at Interfaces. In *Electrochemical Data*; Elsevier Publishing Company: Amsterdam, 1952; p 215.
(54) Gouy, P. M. *Ann. Chim. Phys.* **1906**, *8*, 291.
(55) Busoni, L. An axisymmetric drop shape apparatus for the study of insoluble films. Ph.D. Thesis, University of Florence, 2003.
(56) Spinke, J.; Liley, M.; Guder, H. J.; Angermaier, L.; Knoll, W. *Langmuir* **1993**, *9*, 1821.
(57) Csaeki, A.; Moeller, R.; Straube, W.; Koehler, J. M.; Fritzsche, W. *Nucleic Acids Res.* **2001**, *29*, e81.
(58) Grahame, D. C. *Chem. Rev.* **1947**, *41*, 441.
(59) Leopold, M. C.; Black, J. A.; Bowden, E. F. *Langmuir* **2002**, *18*, 978.
(60) Aoki, K.; Kakiuchi, T. *J. Electroanal. Chem.* **1999**, *478*, 101.
(61) Clasohm, L. Y. A surface force apparatus study of the mercury/water interface with and without self-assembled monolayers. Ph.D. Thesis, University of South Australia, 2005.
(62) Trasatti, S. *Solvent Adsorption and Double-Layer Potential Drop at Electrodes*; Plenum Press: New York, 1979; Vol. 13.